

# Global Table Extractor (GTE): A Framework for Joint Table Identification and Cell Structure Recognition Using Visual Context

Xin Yi Zheng<sup>2</sup>, Douglas Burdick<sup>1</sup>,  
Lucian Popa<sup>1</sup>[0000-0002-0659-9144], and  
Nancy Xin Ru Wang<sup>1</sup>[0000-0002-3041-6934]

<sup>1</sup> IBM Research-Almaden  
{drburdic, lpopa}@us.ibm.com {wangnrxr}@ibm.com  
<sup>2</sup> University of Michigan  
{zxyCarol}@umich.edu

**Abstract.** Documents are often the format of choice for knowledge sharing and preservation in business and science, within which are tables that capture most of the critical data. Unfortunately, most documents are stored and distributed as PDF or scanned images, which fail to preserve table formatting. Recent vision-based deep learning approaches have been proposed to address this gap, but most still cannot achieve state-of-the-art results. We present *Global Table Extractor (GTE)*, a vision-guided systematic framework for joint table detection and cell structured recognition, which could be built on top of any object detection model. With *GTE-Table*, we invent a new penalty based on the natural cell containment constraint of tables to train our table network aided by cell location predictions. *GTE-Cell* is a new hierarchical cell detection network that leverages table styles. Further, we design a method to automatically label table and cell structure in existing documents to cheaply create a large corpus of training and test data. We use this to create SD-Tables and SEC-tables, real-world and complex scientific and financial datasets with detailed table structure annotations to help train and test structure recognition. Our deep learning framework surpasses previous state-of-the-art results on the ICDAR 2013 table competition test dataset in both table detection and cell structure recognition, with a significant 6.8% improvement in the full table extraction system. Further experiments demonstrate a greater than 30% improvement in cell structure recognition F1-score when compared to a vanilla RetinaNet object detection model in our out-of-domain financial dataset (SEC-Tables).

**Keywords:** Document Analysis, Object Detection, Table recognition

## 1 Introduction

In real world enterprise and scientific applications, crucial information is often summarized in tabular form within PDF or scanned documents. Since neither

**A)**

**World Production Capacity:**

	Fused aluminum oxide		Silicon carbide	
	2009	2010	2009	2010
United States and Canada	60,400	60,400	42,600	42,600
Argentina	—	—	5,000	5,000
Australia	50,000	50,000	—	—
Austria	60,000	60,000	—	—
Brazil	50,000	50,000	43,000	43,000
China	700,000	700,000	455,000	455,000
France	40,000	40,000	16,000	16,000
Germany	80,000	80,000	36,000	36,000
India	40,000	40,000	5,000	5,000
Japan	25,000	25,000	60,000	60,000
Mexico	—	—	45,000	45,000
Norway	—	—	80,000	80,000
Venezuela	—	—	30,000	30,000
Other countries	80,000	80,000	190,000	190,000
World total (rounded)	1,190,000	1,190,000	1,010,000	1,010,000

**B)**

Table C1: Summary Statistics  
This table contains summary statistics for 2,012 respondents in SAVE 2009.

Variable	Mean	Std. Dev.	Min	Max
Age	50.8	15.9	21	90
Men	0.47	0.50	0	1
East	0.28	0.45	0	1
Rural	0.15	0.36	0	1
Married	0.57	0.50	0	1
Single	0.21	0.40	0	1
Divorced	0.13	0.33	0	1
Widowed	0.08	0.26	0	1
Separated	0.03	0.16	0	1
Partner	0.65	0.48	0	1
Employed	0.55	0.50	0	1
Fulltime	0.54	0.47	0	1
Parttime	0.20	0.40	0	1
Unemployed	0.08	0.28	0	1
Homemaker	0.19	0.40	0	1
Retired	0.28	0.45	0	1
Household size	2.43	1.22	1	9
Households with children	0.37	0.48	0	1
Number of children	1.67	1.38	0	8

Fig. 1: Tables are challenging to extract as they can be presented in a variety of styles and structures. Graphical ruling lines sometimes do not exist (a) and when present (b), may not be a necessary condition to delineate a cell (red box).

of these widely-used document formats preserve table formatting information, accurate table detection and cell structure recognition techniques are required to reconstruct the table before its contents can be leveraged for any subsequent analysis, such as question answering [24], scientific leaderboard construction [12] or knowledge base population [27]. Accurate table extraction is possibly the most important task and a major pain point in document analysis for businesses where the computer vision community can have a significant impact. In fact, the reliance on rules, lack of labelled data and visual nature of table recognition in documents resembles research in the early days of object recognition in images. *Table detection* refers to detecting the boundary of a table, while *cell structure recognition* generates the logical relations of cells and their contents inside a table, e.g., identification of all cells within the same row or column inside the table. Although straightforward for humans, accurately reconstructing table boundary and cell structure information from PDF or image documents is difficult for automated systems due to the wide variety of styles, layout and content tables have across heterogeneous document sources [11]. Such visual “clues” often conflict across sources, e.g., examples in Figure 1.

Unfortunately, conventional rule-based or statistical techniques for table extraction often fail to generalize as they rely heavily on hand-crafted features like graphical lines or bold font, which are not robust to style variations across different document formats. Compared to these approaches, vision-based deep learning methods have two advantages. First, by working directly on images, they can be applied to any document renderable to an image, including PDF. They do not rely on programmatic PDF encodings such as graphical line, spacing and font attributes which rule-based approaches require. Second, if a large annotated dataset for tables is available, models can be pretrained and then finetuned using a small amount of in-domain labels. Indeed, there are a few vision-based deep learning models for table extraction that have been proposed. However, most existing deep learning approaches directly use off-the-shelf object detectors [26,28,19] without any major architectural adaptation. As a result, such vision-based deep learning models have not yet surpassed traditional non-deep learning methods in all measures [7]. We argue the non-ideal results of deep

learning methods are due to the lack of large-scale dataset, and over-reliance on off-the-shelf object detectors without adaptation to unique properties of tables.

To tackle cell structure recognition, rule-based and statistical machine learning approaches are commonly used [7]. Recent deep learning approaches either output structure as text with a image-to-sequence method [38,19], or generate structure after detecting related objects in the table. Although object detection also needs a box to structure conversion step when compared to end-to-end sequence generation, the visualized bounding boxes of object detection methods are easier for humans to interpret and correct, which leads to better results [11]. Existing work on object detection-based methods detect entire rows and column separately, and represents the intersection of detected rows and columns as cells [28,37]. Such an approach has limitations in accurately detecting structure of complex tables with rows or columns which do not span the entire table or align well. Our proposed Global Table Extractor (GTE) adapts vision-based models to the table identification and cell structure recognition problem, and achieves state-of-the-art results by addressing limitations of existing work as follows. First, GTE improves object detectors by explicitly enforcing the model to learn the natural constraint of tables: A table must contain certain amount of cells inside it and a cell cannot exist outside of the table. In other words, the model should not only focus on the tables, but also pay attention to the cells inside. Second, we propose to detect each cell directly instead of detecting entire rows and columns separately since cells are more visually distinct as object units and this approach naturally supports tables with rows and columns not spanning the entire table. Third, current object detection models focus on the local area around objects, which neglects the global style of tables that determine cell appearance. To leverage the information of the whole table, we propose a hierarchical system of networks where we discriminate the global context first, the table style. The table image is then fed into different object detectors specialized for different styles. After cell bounding boxes are detected, we invent a cell cluster-based algorithm to generate cell structures.

In summary, our contributions are as follows:

1. We present our systematic framework for vision-guided joint table detection and cell structure recognition, GTE, which outperforms previous systems on the ICDAR 2013 table competition benchmark. We also show more than 30% accuracy improvements testing on an out-of-domain dataset when compared to naive object detection networks trained with but not adapted for tables. We are currently undergoing an internal process to open source the code.
  - (a) We leverage a cell detection network to guide the training of the table detection network.
  - (b) We present a hierarchical network and a novel cluster-based algorithm for cell structure recognition by classifying tables, detecting cells and convert this into structure with spatial clustering.
2. We design a method to automatically create ground-truth labels for table recognition and use it to create SD-Tables and SEC-Tables, which are large datasets from real-world data sources with fine-grained cell structure annotation for table related tasks. We intend to make SD-Tables and SEC-Tables

(subject to legal evaluations) publicly available to address the lack of such labelled data, which is useful for training deep-learning based models.

## 2 Related Work

### 2.1 Table Detection

Rule-based methods were among the earliest proposed approaches for locating tables inside a document [8,10,13,4,29]. Such rules mainly focus on text-block arrangement, horizontal and vertical lines, and item blocks. Rule-based systems perform well on some documents, but require extensive human effort to summarize rules and often fail to generalize to other domains or across heterogeneous table formats. Statistical machine learning approaches have been proposed to fill these gaps. Unsupervised methods use bottom-up clustering of word segments [18]. Examples of supervised methods include learning a MXY tree to represent a table [1], learning a Hidden Markov Model designed for table structure [35] and learning a SVM to classify tables using line information [15]. Semi-supervised methods have also been proposed to leverage unlabelled documents [2]. Recently, data-driven vision based approaches have been used to detect tables by adapting state-of-the-art object detectors such as Faster-RCNN to table detection [28,19,5].

### 2.2 Cell Structure Recognition

Earliest successful system is the rule-based T-RECS by evaluating horizontal and vertical structure of words [18]. Wang et al. presented a seven-step process similar to the X - Y cut algorithm to improve the previous system with statistical learning approaches from a training corpus [39]. Shigarov et al. decomposed tables by offering configuration of algorithms, thresholds and rule sets based on PDF metadata [31]. Recently, there is a trend from rule-based and statistical machine learning to deep learning methods in table recognition. Deep learning approaches include two categories: (a) End-to-end image-to-sequence models [19]; (b) Object detection based methods [28,37].

### 2.3 Existing Datasets

During the development of GTE, we found few existing datasets with any kind of structure annotation. We required a dataset with a large number of labelled examples where each table cell is annotated with its pixel-coordinate location, logical coordinates inside the table structure (e.g., row-span and col-span) and cell text contents. Although the ICDAR2013 dataset met the annotation requirements, only 254 table examples (96 train and 156 test from the competition) were available, which were from European Union and US Government reports [7]. TableBank has 145K labelled tables, but provides only logical coordinates of cells in the table [19]. While in our SD-Tables dataset, annotations give detailed information on the logical structure as well as the location and contents of each

cell, similar to the ICDAR2013 competition. Very recently, a new ICDAR2019 table competition was held with not PDF files but images of document pages. It contains in total 80 documents for table structure recognition, including both modern and handwritten archival documents. They do not have a training set for modern documents, only some for testing. Other existing datasets only contain table boundary information [30,34].

### 3 SD-Tables & SEC-Tables Datasets

As shown above, there is a lack of large scale datasets for cell structure recognition. To fill this gap, we designed a novel method to automatically match PDF and HTML documents in order to generate a large and comprehensive table recognition dataset. We source these from open-access scientific documents in the Science Direct repository. To generate the cell structure labels, we use token matching between the PDF and HTML version of each article. From the HTML, we know the logical structure of the table cells and from the PDF, we know the cell and table boundary location. There are sometimes token matching errors due to the same tokens in multiple locations or token encoding differences so we also manually verify and correct some articles in the dataset. SD-Tables contains more than 450 documents from more than 28 scientific disciplines and hundreds of journals with more than 1000 tables and 180K cells annotated. To combat the over-similarity of table styles in Science Direct, we collected articles from the full range of scientific disciplines, from humanities to medicine to engineering. As well, whenever possible, we use the PDF version that was uploaded at the time of acceptance, before the format standardization process.

On top of this training dataset, we also created 2 test sets to capture complex tables from real world sources. One is from the same Science Direct repository, consisting of 191 tables. To test if our model is able to perform on out-of-domain documents without retraining, we also sourced from annual reports of public financial filings to create a set of 244 tables that we have named SEC-Tables. Financial tables often have very different styles when compared to ones in scientific and government documents, with fewer graphical lines and larger gaps within each table and more colour variations.

## 4 Methods

As shown in Figure 2, our full GTE framework consists of a series of vision-based neural networks. Each of the main object detection networks use context from the output of the other networks. The framework could be adapted to any kind of object detector. The table boundary network (GTE-Table) uses a cell detection network by leveraging the fact that tables must contain at least some cells. The cell structure recognition network (GTE-Cell) uses table boundaries from the table boundary network (GTE-Table) and table-level style information (Attributes Net).

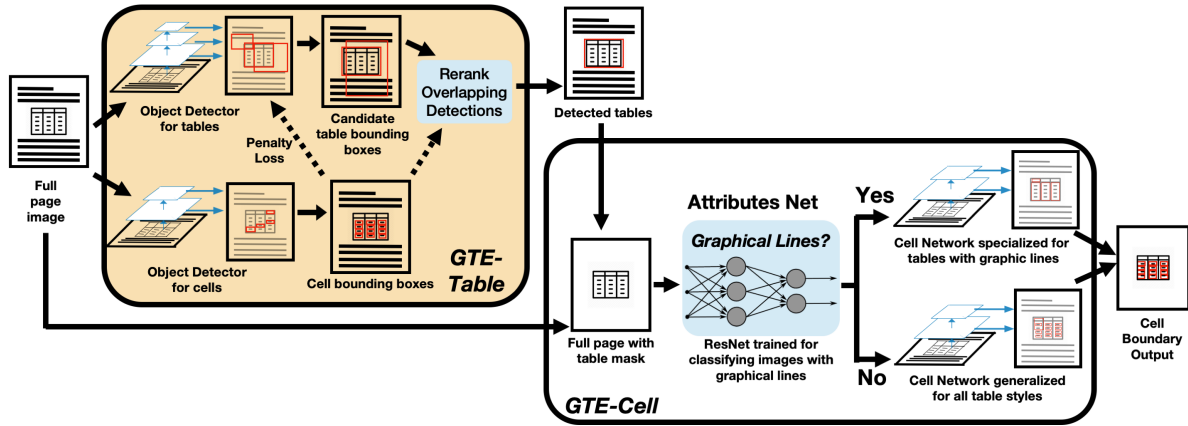
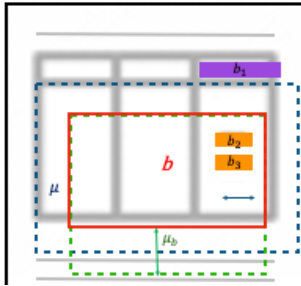


Fig. 2: Our full GTE Framework consists of several networks for table (GTE-Table) and cell (GTE-Cell) boundary detection. The input is an image form of a document page for both sub-frameworks, but note GTE-Cell depends on table boundaries output by GTE-Table to generate cell structures for each specific table.

#### 4.1 GTE-Table

- (1) Let Bounding box  
 $b = \{(x_1, y_1), (x_2, y_1), (x_1, y_2), (x_2, y_2)\}$   
 (2) Let a set of bounding boxes  
 $B = \{b_i | i=1,2,3\}$



Then:

- (1) Operator  $M(B)$ : binary mask of bounding box(es)  $B$ ;  
**Orange and Purple area is 1, else 0**

- (2) Operator  $A(b) = (x_2 - x_1) \cdot (y_2 - y_1)$ :  
 Area of  $b$

- (3) Operator  $SLC(M(B), b) = \sum_{x=x_1}^{x_2} \sum_{y=y_1}^{y_2} M(B)_{x,y}$   
 Area of overlap between mask  $M(B)$  and box  $b$ ; **Orange area**

- (4) Operator  $S(b, \mu) = (x_1 - \mu, x_2 + \mu, y_1 - \mu, y_2 + \mu)$   
 Enlarge box  $b$  by  $\mu$  pixels; **Blue box**

- (5) Operator  $U(b, \mu_b) = (x_1, x_2, y_1, y_2 + \mu)$   
 Enlarge the bottom of box  $b$  by  $\mu$  pixels; **Green box**

Fig. 3: Definition of Operators used in Sec 4.1.

In the training stage, besides the regression and classification loss, we add a piecewise constraint loss. It penalizes the detection probability of unrealistic tables when considering cell locations. This novel cell constraint based loss function may be added to any detection network. We formalize the terminologies of this section here. We make the following definitions in Fig. 3.

We used the guided cell network to generate a set of cell bounding box(es)  $B_{cells} = \{b_{cell,i} | i\}$ . The cells are detected by a simpler non-hierarchical version of our GTE-Cell network that is trained on only original full-page document pages, without knowing the location of the tables. Given  $B_{cells}$ , we define two Boolean operators where inputs are an inner box ( $b_{ibox}$ ) and outer box ( $b_{obox}$ ), which define

the boundaries of the mask input area:

$$C(b_{ibox}, b_{obox}) = \left\{ \begin{aligned} &SLC(M(B_{cells}), b_{obox}) - SLC(M(B_{cells}), b_{ibox}) \\ &< \left\{ \alpha \cdot (A(b_{obox}) - A(b_{ibox})) \right\} \end{aligned} \right\} \quad (1)$$

$$D(b_{ibox}, b_{obox}) = \left\{ SLC(M(B_{cells}), b_{obox}) - SLC(M(B_{cells}), b_{ibox}) \right\} > 0 \quad (2)$$

Where C is true if the area covered by the cells between  $b_{obox}$  and  $b_{ibox}$  is at most alpha times the area of the  $b_{obox}$  minus area of the  $b_{ibox}$ . D is true if any cells exist in the area between  $b_{ibox}$  and  $b_{obox}$ . The penalty indicator  $I(b_{tbl})$  is defined as

$$I(b_{tbl}) = C((0, 0, 0, 0), b_{tbl}) \vee C(S(b_{tbl}, \mu_1), b_{tbl}) \vee D(S(b_{tbl}, \mu_2), S(b_{tbl}, \mu_3)) \vee C(U(b_{tbl}, \mu_4), b_{tbl}) \quad (3)$$

The penalty indicator is true when any of the following conditions are true:

- $C((0, 0, 0, 0), b_{tbl})$  : Less than  $\alpha$  of the whole table has cells.
- $C(S(b_{tbl}, \mu_1), b_{tbl})$  : Less than  $\alpha$  of the area just inside the table has cells.
- $D(S(b_{tbl}, \mu_2), S(b_{tbl}, \mu_3))$ : The area just outside of the table contains any cells.
- $C(U(b_{tbl}, \mu_4), b_{tbl})$ : Less than  $\alpha$  of the area at just inside the bottom of the table has cells.

Then the constraint loss( $CL$ ) is

$$\sum_{b_{tbl}}^{B_{tbl}} I(b_{tbl})P(b_{tbl}) + \gamma_1(1 - I(b_{tbl}))(1 - P(b_{tbl})) \quad (4)$$

where  $P(\cdot)$  is the table detection probability function. We choose  $\mu_1 = -5$ ,  $\mu_2 = 5$ ,  $\mu_3 = 10$ ,  $\mu_4 = -10$ ,  $\alpha = 1/8$ ,  $\gamma_1 = 1/10$  in our experiments. Additionally, one of the input image channels to the table network is replaced with a mask generated from the prediction of cells to further aid training.

In the inference stage, instead of the widely used non-max suppression, our ranking of proposed bounding boxes not only consider detection probabilities, but also the presence of cells inside and outside the table. We define **Constraint Coefficient**( $CCcoef$ ) for each bounding box, where

$$CCcoef(b_{tbl}) = SLC(M(B_{cell}), S(b_{tbl}, \mu_5)) - SLC(M(B_{cell}), b_{tbl}) - \gamma_2 \cdot (SLC(M(B_{cell}), b_{tbl}) - SLC(M(B_{cell}), S(b_{tbl}, \mu_6))) \quad (5)$$

For each boundary of the table bounding box, we calculate the amount of cells just outside subtracted by the amount of cells just inside the table. For any pair of bounding boxes  $b_i, b_j$  overlapped with each other more than  $\delta\%$ , and  $|P(b_i) - P(b_j)| < \epsilon$ , we discard the bounding box with higher  $CCcoef$ . We choose  $\mu_5 = -20$ ,  $\mu_6 = \{0.25 * (x_2 - x_1), 0.25 * (y_2 - y_1)\}$ ,  $\gamma_2 = 0.1$ ,  $\epsilon = 0.1$ ,  $\delta = 25$  in our experiments. We will in detail describe the hyper-parameter selection in Experiment Setup.



Therefore, cells that start with a small case is likely a case of over-splitting. We merge these cells with the cell above. Also, we perform some post-processing steps. This includes assigning locations to leftover text boxes that were not overlapping with any detected cells and we split cells in certain cases when there are gaps nearby. Before producing the final logical structure of each cell in the table, we increase the row and column span of cells when the text box intersects with neighboring empty rows or columns as this is likely a hierarchical cell spanning multiple rows or columns. Our clustering-based algorithm is more efficient than a greedy or exhaustive search method that selects each cell sequentially. As well, many of our steps are designed to be robust against cell detection errors. For more details, see Algorithm 1 in the supplementary material.

Table 1: Table Detection Percent Results on ICDAR2013. We also provide purity and completeness scores when available. There are a few other methods[33,14,16] that could not be compared directly in this table as they are using a measure based on Intersection-over-union(IOUS) where the IOU threshold=0.5. Our method achieves F1=0.997 by this measure, which is higher than reported by the other methods. We observe the character-based measure computed by the competition script better measures table quality than a measure based on IOU threshold of 0.5, since the latter counts as correct for predictions capturing only half of a ground-truth table which have little practical use.

Category	Method	Input type	Recall	Precision	F1	Cpt	Pu
Commercial Softwares	<i>FineReader</i>	PDF	99.71	97.29	98.48	142	148
	<i>OmniPage</i>	PDF	96.44	95.69	96.06	141	130
	<i>Nitro</i>	PDF	93.23	93.97	93.60	124	144
	<i>Acrobat</i>	PDF	87.38	93.65	90.40	110	141
Non Deep Learning	<i>ICST-Table</i> [3]	PDF	26.97	74.96	39.67	28	41
	<i>TableSeer</i> [23]	PDF	33.35	88.36	48.64	0	29
	<i>Nurminen</i> [7]	PDF	90.77	92.10	91.43	114	151
	<i>TABFIND</i> [36]	PDF	98.31	92.92	95.54	149	137
	<i>pdf2table</i> [40]	PDF	85.30	63.99	73.13	100	94
	<i>TEXUS</i> [25]	PDF	90.23	88.32	89.26	114	138
Deep Learning	<i>Hao</i> [9]	Image	97.24	92.15	94.63	/	/
	<i>DeepDeSRT</i> [28]	Image	96.15	97.40	96.77	/	/
	<i>TableBank</i> [19]	Image	/	/	96.25	/	/
Ours	GTE	Image	98.82	99.93	<b>99.25</b>	146	146

## 5 Experiments

### 5.1 Datasets

We perform our experiments on both the table detection and cell structure recognition tasks in the widely used ICDAR2013 table competition [7]. This

dataset is considered as the standard benchmark dataset in PDF table extraction. It contains 96/156 tables for training/testing collected from European Union and US Government reports. Since the in-domain dataset is very small, pretraining the model on other datasets is required. For table detection, we pretrain the model on the combination of TableBank([19]) and SD-Tables; For cell structure recognition, we pretrain the model on SD-Tables.

We also conduct additional experiments on the SD-Tables test set and the SEC-Tables dataset. As our model is not trained on financial filing data, it can be considered out-of-domain results.

## 5.2 Evaluation Metrics

We follow the official evaluation metrics of ICDAR2013 table competition [7]. For table detection, the metrics are character-level Recall (Rec.), Precision (Prec.) and F1-measure  $op(F1)$ , averaged per document, along with Purity (Pu) and Completeness (Cpt). They are defined as follows:

$$Pu = \sum_{n \in N} [Rec(n)] \quad Cpt = \sum_{n \in N} [Prec(n)]$$

Where  $N$  is the set of test documents.

For cell structure recognition, the metrics are precision, recall and F1-measure for generated adjacency matrices. Additional details are available in [6] and [7].

## 5.3 Experimental Setup

**Training and Inference Details** We leverage TableBank and SD-Tables table boundary to pretrain the object detection network before fine-tuning on the ICDAR train set for the table boundary detection task[21]. We use the architecture of RetinaNet with Resnet50-FPN backbone as our base object detection model [21,20]. We use resolution of 643 by 900 for tables, and 965 by 1350 for cells, as cells need higher resolutions to distinguish. We redesigned the feature pyramid network for tables and cells such that there are fewer detection layers than a typical object detection network but this allows for finer-grained anchor boxes for cells and larger object boxes for tables without sacrificing computational efficiency. We add anchors with aspect ratio 0.1 and 0.25 for each feature map to catch commonly appearing wide tables and cells. In the cell network, since the objects are really dense, we use anchors of sizes 0.5, 0.7, 1, 1.2, 1.6 of the set of aspect ratio anchors. We add additional smaller scale anchors because many cells are much smaller than the anchors. In the table network, we run each page at test time at multiple zoom scales to help improve detection of abnormally small or large tables. These are at 95%, 90%, 105% and 110%. All the object detection models in GTE are initialized with the parameters pretrained on MS COCO dataset [22].

**Hyper-parameter Selection** For joint training, our hyper-parameters are selected from characteristics of the ICDAR training data. On average, the height of a character is 10 pixels. We wanted to check the text density of tables just inside and just outside of the table; we chose 5 pixels (or half a character height) for this purpose. As a result, we chose  $\mu_1 = 5$  and  $\mu_2 = 5$  in Eq.3. We also chose  $\alpha = 1/8$  (the density threshold) in Eq.1: we calculated the cell density of tables in the training set and found that the value at the lower end of the density scale (5th percentile) was around  $1/8$ . We did not select the minimum (which was around 0.1) in case there are outliers in the training set. Finally,  $\gamma_1 = 1/10$  in Eq.4 gives less penalty to false negative bounding boxes to better reflect the proportion between false positive and false negative bounding boxes (as we found that an equal penalty caused the iterative training to become unstable very quickly).

For inference time, we found there may be overlapping tables that can be quite different in shape while having similar confidence levels. Thus, we choose a set of parameters ( $\mu_5, \mu_6, \gamma_2, \epsilon, \delta$ ) to prioritize tables with the most tabular characteristics. In particular, we prioritize tables not having any cells within 2 lines of text outside the table ( $\mu_5 = -20$  pixels), while having many cells just inside the table, up to 0.25 of area (i.e.,  $\mu_6 = \{0.25 * (x_2 - x_1), 0.25 * (y_2 - y_1)\}$  pixels).

## 5.4 Experimental Results

**Table Detection** As reported in Table 1, GTE-Table achieves the best character-level F1 measure among all methods. Although *FineReader* slightly outperforms GTE on purity, the higher F1-measure for GTE indicates GTE produces higher quality boundaries closer to ground-truth. Since the purity metric penalizes all incorrect table boundaries equally, it does not provide “partial-credit” for almost correct answers in the same manner as character F1-measure for cases where the predicted boundary only includes a few extra characters. Figure 4 shows some correctly detected table boundaries as well as some failures. In general, we see three types of errors, partial under-detection, where some parts of the ground truth table is missing, partial over-detection, where some text outside of the ground truth is mistakenly included and mis-detection, where a non-table entity such as a chart was misidentified as a table. We do not see any cases of table non-detection in our ICDAR2013 test results and only one case of mis-detection. Overall, most partial detections are only missing or adding one or two extra lines, such as a short captions in the table.

**Table Detection Ablation Study** As shown by the additional experimental results in Table 2, the base detection network trained to perform the cell and table detection task simultaneously (Detection-base) performs far worse than the more specialized networks. There are two main reasons behind this. First, TableBank data cannot be leveraged when pretraining the networks because it lacks cell bounding boxes annotations [19] so it is only trained of SD-tables and fine-tuned on ICDAR training data. Second, tables and cells are of two completely different scales where it is hard to choose an appropriate resolution to generate

Table 2: Table detection additional experiments with percent results.

Method	Rec.	Prec.	F1	Cpt	Pu
Detection-Base	85.90	81.51	78.38	85	69
GTE-Table-Sep	96.91	95.64	95.87	143	126
GTE-Table-Joint	97.92	99.71	98.61	141	146
GTE-Table-Joint w/ reranking and multi-zoom	98.82	99.93	<b>99.25</b>	146	146

anchors fitting the two scales. On the other hand, it is still important for the cell network and table network to leverage each other’s information, as shown by the nearly 3% boost in F1 accuracy as compared to the regular object detection losses (GTE-Table-Sep) that do not use information from other networks. Finally, combining table detections from zoomed in and out versions of the document page and then reranking these detections with the cell network output slightly improves accuracy.

	THRESHOLD FOR RELEASES		
	to air kg/year	to water kg/year	to land kg/year
Asbestos	1	1	1
Chlorides (as total Cl)	-	2 million	2 million
Cyanides (as total CN)	-	50	50
Fluorides (as total F)	-	2 000	2 000
Particulate matter (PM10)	50 000	-	-
Total Nitrogen	-	50 000	50 000
Total Phosphorus	-	5 000	5 000

	THRESHOLD FOR RELEASES		
	to air kg/year	to water kg/year	to land kg/year
Asbestos	1	1	1
Chlorides (as total Cl)	-	2 million	2 million
Cyanides (as total CN)	-	50	50
Fluorides (as total F)	-	2 000	2 000
Particulate matter (PM10)	50 000	-	-
Total Nitrogen	-	50 000	50 000
Total Phosphorus	-	5 000	5 000

Fig. 5: Partial cell detections with correct cell structure

**Cell Structure Recognition** As reported in Table 3, GTE-Cell outperforms all previous methods and commercial software in all metrics even without using any PDF encodings (ruling lines, rendering techniques, etc). All results are from cell detection on outputs produced from table detection by each framework, not the ground truth table. When analyzing the qualitative results in Figure 5, we see cell boundary detection often generates a detection box that is too short for very long lines of text. This is a key limitation of the anchor-based object detection system, which has difficulties with aspect ratios differing greatly from ones in the configuration. As well, in the case of tables without graphical lines at every row and column, the model may mistakenly merge multiple cells into one. In many cases, our post-processing boundary to structure algorithm is robust to some of these mistakes are still able to generate a correct or nearly correct structure output. We see three main types of detection errors that can lead to incorrect structure output. There are overmerged cell detection, where two or more cells are incorrectly merged together, oversplit cell detection, where one cell has been incorrectly split into multiple cells and cell non-detection, where there is no predicted bounding box that includes such a cell. These errors can lead to a number of inaccuracies in the boundary to cell structure process, including

incorrect number of rows and columns, alignment and of course final cell location assignment as well. Examples of such errors are in the supplementary material.

Table 3: Cell Structure percent results on ICDAR2013 show that GTE improves previous state-of-the-art in cases where the ground truth table border (GT Border) was and was not used. To note, our F1-score is also higher than that of three other related methods, but they could not be compared directly in this table. DeepDeSRT[28] and DeepTabStr[32] split the ICDAR2013 test set into two parts, leaving only 31 of 156 tables for testing and the rest incorporated into training. To the best of our ability, we have not found which 31 tables were selected. [31] presented in the paper that they used a different evaluation script, so it is not directly comparable to other numbers reported in ICDAR2013 table competition.

Category	Method	GT Border?	Rec.	Prec.	F1
Commercial Softwares	<i>FineReader</i>	N	88.35	87.10	87.72
	<i>OmniPage</i>	N	83.80	84.60	84.20
	<i>Nitro</i>	N	67.93	84.59	75.35
	<i>Acrobat</i>	N	72.62	81.59	76.85
Academic Systems	<i>Nurminen</i> [7]	N	80.78	86.93	83.74
	<i>TEXUS</i> [25]	N	84.23	81.02	82.59
	<i>KYTHE</i> [7]	N	48.11	57.40	52.20
	<i>pdf2table</i> [40]	N	59.51	57.52	58.50
	<i>TABFIND</i> [36]	N	70.52	68.74	69.62
Ours	GTE	N	94.70	94.49	<b>94.57</b>
Academic Systems	<i>Tensmeyer</i> [37]	Y	94.64	95.89	95.26
	<i>Nurminen</i> [7]	Y	94.09	95.12	94.60
	<i>Khan</i> [17]	Y	90.12	96.92	93.39
	<i>TABFIND</i> [36]	Y	64.01	61.44	62.70
Ours	GTE	Y	95.74	95.39	<b>95.55</b>

**Cell Structure Ablation Study** To analyze our GTE-Cell network further, we compare the several variations in Table 4 using ground truth table borders. Firstly, the baseline detection network (Detection-Base) that performs both cell and table detection has very poor recall and precision. For networks specialized for cell detection, we see that the model pretraining on the SD-Tables dataset gives a boost when compared to GTE-Cell-Style-Mix-Train-no-sd. We also test each of the sub detection networks (GTE-Cell-Style-Mix-Train for the network trained on all augmentations and GTE-Cell-Border-Train trained on original and graphical line augmentations). The full hierarchical model (GTE-Cell-Hierarchical) performs better than both individual sub-models, showing that it is indeed helpful to first determine the style of the table and then use the model trained on data most similar to it. Out of 156 total test tables in ICDAR2013, there are 108 with at least some vertical graphical lines (69.23%). To note, our attributes network

(graphical line table classifier) was correct in 123 out of 156 tables (78.84%). The errors generally come from very small tables or tables with vertical graphical lines that only span the header, which is an ambiguity also present in the training data. To help mitigate this error, during the row and column sampling step, we keep track of the standard deviation of the sampling points. If this value is high, it likely indicates that the cell detection model used was not suitable for the given table as tables tend to have similar number of columns and rows throughout, thus we would then use the alternate cell model.

Table 4: Cell structure additional experiments with percent results using ground truth table borders.

Method	Rec.	Prec.	F1
Detection-Base	78.68	74.07	75.82
GTE-Cell-Style-Mix-Train-no-sd	89.78	89.30	89.43
GTE-Cell-Style-Mix-Train	93.27	93.12	93.15
GTE-Cell-Border-Train	91.30	89.65	90.31
GTE-Cell-Hierarchical	95.74	95.39	<b>95.55</b>

**Experiments with Additional Datasets** To demonstrate the robustness of our network on more complex tables and ones outside of the training data domain, we tested the same model on SD-Tables test set and SEC-Tables (Table 5). We show that although these tables are more complex as they rarely have any graphical separation lines, our model is still able to detect the tables and its structure with high accuracy. Additionally, although financial filings were not part of the training set, we still demonstrate good performance on these out-of-domain documents. In particular, there is at least a 30% improvement in cell structure recognition when compared to the base object detection model. Finally, one may note that there is not a large difference between GTE-Table and Detection-Base for SD-Tables, likely due to the uniform size and look of tables from scientific articles. However, there is still a significant difference when it comes to the cell structure. This shows that both GTE-Table and GTE-Cell play important roles in our state-of-the-art table structure recognition performance.

## 6 Conclusion and Future Work

In summary, we have demonstrated a vision based table extraction framework with state-of-the-art results. It can perform the full pipeline of table recognition, from document to table structure, which can be used easily for down-stream analysis. Our framework leverages the global visual context of tables, including the style and rules in the relationship between cells and tables. As well, we will release our SD-Tables dataset, which we hope will help others using data hungry

Table 5: Table detection and cell structure (with table detection output for boundary) results on SD-Tables (Scientific Papers) and out-of-domain (OOD) SEC-Tables (Financial Filings).

Dataset	Table Method	Rec.	Prec.	F1	Cell Method	Rec.	Prec.	F1
SD-Tables	<i>Detection-Base</i>	93.37	93.76	92.74	<i>Detection-Base</i>	71.41	70.80	69.88
	<i>GTE-Table</i>	93.87	95.09	<b>94.10</b>	<i>GTE-Cell</i>	76.51	81.66	<b>78.41</b>
SEC-Tables (OOD)	<i>Detection-Base</i>	45.61	56.76	47.76	<i>Detection-Base</i>	41.58	33.89	36.05
	<i>GTE-Table</i>	92.43	78.40	<b>82.00</b>	<i>GTE-Cell</i>	73.82	63.37	<b>67.47</b>

methods to tackle table-related problems. Our vision based method is very easily merged with Optical Character Recognition (OCR) methods to perform table recognition fully from images.

## References

1. Cesarini, F., Marinai, S., Sarti, L., Soda, G.: Trainable table location in document images. Object recognition supported by user interaction for service robots **3**, 236–240 vol.3 (2002)
2. Fan, M., Kim, D.S.: Table region detection on large-scale PDF files without labeled data. CoRR [abs/1506.08891](https://arxiv.org/abs/1506.08891) (2015)
3. Fang, J., Gao, L., Bai, K., Qiu, R., Tao, X., Tang, Z.: A table detection method for multipage pdf documents via visual separators and tabular structures. 2011 International Conference on Document Analysis and Recognition pp. 779–783 (2011)
4. Gatos, B., Danatsas, D., Pratikakis, I., Perantonis, S.J.: Automatic table detection in document images. In: ICAPR (2005)
5. Gilani, A., Qasim, S.R., Malik, M.I., Shafait, F.: Table detection using deep learning. 2017 14th IAPR International Conference on Document Analysis and Recognition (ICDAR) **01**, 771–776 (2017)
6. Göbel, M.C., Hassan, T., Oro, E., Orsi, G.: A methodology for evaluating algorithms for table understanding in pdf documents. In: ACM Symposium on Document Engineering (2012)
7. Göbel, M.C., Hassan, T., Oro, E., Orsi, G.: Icdar 2013 table competition. 2013 12th International Conference on Document Analysis and Recognition pp. 1449–1453 (2013)
8. Green, E.J., Krishnamoorthy, M.S.: Recognition of tables using grammars (1995)
9. Hao, L., Gao, L., Yi, X., Tang, Z.: A table detection method for pdf documents based on convolutional neural networks. 2016 12th IAPR Workshop on Document Analysis Systems (DAS) pp. 287–292 (2016)
10. Hirayama, Y.: A method for table structure analysis using dp matching. Proceedings of 3rd International Conference on Document Analysis and Recognition **2**, 583–586 vol.2 (1995)
11. Hoffswell, J., Liu, Z.: Interactive repair of tables extracted from pdf documents on mobile devices. In: CHI (2019)
12. Hou, Y., Jochim, C., Gleize, M., Bonin, F., Ganguly, D.: Identification of tasks, datasets, evaluation metrics, and numeric scores for scientific leaderboards construction. arXiv preprint [arXiv:1906.09317](https://arxiv.org/abs/1906.09317) (2019)
13. Hu, J., Kashi, R.S., Lopresti, D.P., Wilfong, G.T.: Medium-independent table detection. In: Document Recognition and Retrieval (1999)
14. Huang, Y., Yan, Q., Li, Y., Chen, Y., Wang, X., Gao, L., Tang, Z.: A yolo-based table detection method. In: 2019 International Conference on Document Analysis and Recognition (ICDAR). pp. 813–818 (2019)
15. Kasar, T., Barlas, P., Adam, S., Chatelain, C., Paquet, T.: Learning to detect tables in scanned document images using line information. In: 2013 12th International Conference on Document Analysis and Recognition. pp. 1185–1189 (Aug 2013)
16. Kavasidis, I., Palazzo, S., Spampinato, C., Pino, C., Giordano, D., Giuffrida, D., Messina, P.: A saliency-based convolutional neural network for table and chart detection in digitized documents. ArXiv [abs/1804.06236](https://arxiv.org/abs/1804.06236) (2018)
17. Khan, S.A., Khalid, S.M.D., Shahzad, M.A., Shafait, F.: Table structure extraction with bi-directional gated recurrent unit networks. In: 2019 International Conference on Document Analysis and Recognition (ICDAR). pp. 1366–1371. IEEE (2019)
18. Kieninger, T., Dengel, A.: The t-recs table recognition and analysis system. In: Document Analysis Systems (1998)

19. Li, M., Cui, L., Huang, S., Wei, F., Zhou, M., Li, Z.: Tablebank: Table benchmark for image-based table detection and recognition. ArXiv **abs/1903.01949** (2019)
20. Lin, T.Y., Dollár, P., Girshick, R.B., He, K., Hariharan, B., Belongie, S.J.: Feature pyramid networks for object detection. 2017 IEEE Conference on Computer Vision and Pattern Recognition (CVPR) pp. 936–944 (2016)
21. Lin, T.Y., Goyal, P., Girshick, R.B., He, K., Dollár, P.: Focal loss for dense object detection. 2017 IEEE International Conference on Computer Vision (ICCV) pp. 2999–3007 (2017)
22. Lin, T.Y., Maire, M., Belongie, S.J., Bourdev, L.D., Girshick, R.B., Hays, J., Perona, P., Ramanan, D., Dollár, P., Zitnick, C.L.: Microsoft coco: Common objects in context. In: ECCV (2014)
23. Liu, Y., Bai, K., Mitra, P., Giles, C.L.: Tableseer: automatic table metadata extraction and searching in digital libraries. In: JCDL (2007)
24. Pasupat, P., Liang, P.: Compositional semantic parsing on semi-structured tables. In: ACL (2015)
25. Rastan, R., Paik, H.Y., Shepherd, J.: Texus: A task-based approach for table extraction and understanding. In: DocEng (2015)
26. Ren, S., He, K., Girshick, R.B., Sun, J.: Faster r-cnn: Towards real-time object detection with region proposal networks. IEEE Transactions on Pattern Analysis and Machine Intelligence **39**, 1137–1149 (2015)
27. Rotmensch, M., Halpern, Y., Tlimat, A., Horng, S., Sontag, D.: Learning a health knowledge graph from electronic medical records. Scientific reports **7**(1), 1–11 (2017)
28. Schreiber, S., Agne, S., Wolf, I., Dengel, A., Ahmed, S.: Deepdesrt: Deep learning for detection and structure recognition of tables in document images. 2017 14th IAPR International Conference on Document Analysis and Recognition (ICDAR) **01**, 1162–1167 (2017)
29. Shafait, F., Smith, R.: Table detection in heterogeneous documents. In: Document Analysis Systems (2010)
30. Shahab, A., Shafait, F., Kieninger, T., Dengel, A.: An open approach towards the benchmarking of table structure recognition systems. In: Document Analysis Systems (2010)
31. Shigarov, A.O., Mikhailov, A.A., Altaev, A.: Configurable table structure recognition in untagged pdf documents. In: DocEng (2016)
32. Siddiqui, S.A., Fateh, I.A., Rizvi, S.T.R., Dengel, A., Ahmed, S.: Deeptabstr: Deep learning based table structure recognition. In: 2019 International Conference on Document Analysis and Recognition (ICDAR). pp. 1403–1409. IEEE (2019)
33. Siddiqui, S.A., Malik, M.I., Agne, S., Dengel, A., Ahmed, S.: Decnt: Deep deformable cnn for table detection. IEEE Access **6**, 74151–74161 (2018)
34. Siegel, N., Lourie, N., Power, R., Ammar, W.: Extracting scientific figures with distantly supervised neural networks. In: JCDL (2018)
35. Silva, A.C.e.: Learning rich hidden markov models in document analysis: Table location. In: Proceedings of the 2009 10th International Conference on Document Analysis and Recognition. pp. 843–847. ICDAR '09 (2009)
36. Silva, A.C.e.: Parts that add up to a whole: a framework for the analysis of tables. PH.D. dissertation, The University of Edinburgh (2010)
37. Tensmeyer, C., Morariu, V.I., Price, B., Cohen, S., Martinez, T.: Deep splitting and merging for table structure decomposition. In: 2019 International Conference on Document Analysis and Recognition (ICDAR). pp. 114–121. IEEE (2019)
38. Vinyals, O., Toshev, A., Bengio, S., Erhan, D.: Show and tell: A neural image caption generator. 2015 IEEE Conference on Computer Vision and Pattern Recognition (CVPR) pp. 3156–3164 (2014)

39. Wang, Y., Phillips, I.T., Haralick, R.M.: Table structure understanding and its performance evaluation. *Pattern Recognition* **37**, 1479–1497 (2004)
40. Yildiz, B., Kaiser, K., Miksch, S.: pdf2table: A method to extract table information from pdf files. In: *IICAI* (2005)

# 1 Visualization of different structure format

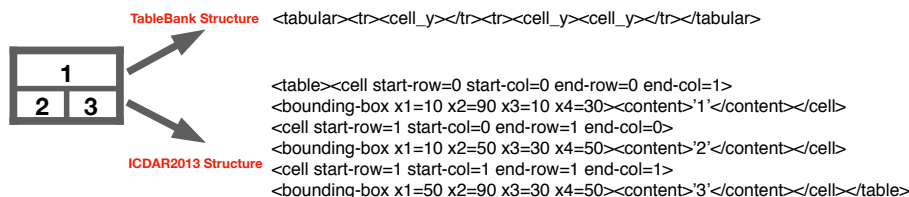


Figure 1: TableBank versus ICDAR2013 structure annotations

## 2 Experimental Details

### 2.1 GTE-Table Network

We make a few changes to the original RetinaNet model in GTE-Table. We add anchors with aspect ratio  $\{0.1, 0.25\}$  to each feature map for wide tables. The input image size is  $900 * 643$ .

### 2.2 GTE-Cell Network

The GTE-Cell Network is composed of a line classifier network at the top of the hierarchy and two object detection models that specialize on different styles of tables. The graphic line classifier network is a ResNet50 model with a binary classifier on top. This network is first pretrained with the attributes derived from SD-Tables dataset and then fine-tuned on the ICDAR train dataset. The ground truth data is derived from the presence of nearby vertical graphical lines (as detected by a PDF parser) for each cell. We make the following changes to the original RetinaNet model in GTE-Cell for cell object detection. Since the scale of cell is generally small, we use pyramid levels  $P3$  and  $P5$ . We find that skipping  $P4$  allows us to add additional anchors while keeping a similar level of computational efficiency. We add anchors with aspect ratio  $\{0.1, 0.25\}$  to each feature map to better detect very wide cells. For denser scale objects, at each level we use anchors of sizes  $\{0.5, 0.7, 1, 1.2, 1.6\}$  of the set of aspect ratio anchors. We add additional smaller scale anchors because the majority of cells are much smaller than the anchors generated from  $P3$ . The input image size is  $965 * 1350$ .

## 3 Cluster-based Algorithm for Generating Cell Structure

---

**Algorithm 1** Cell Boundary to Structure Cluster Algorithm

---

```
1: procedure PREPROCESS CELL BOUNDING BOXES
2:   for  $b$  in  $cellboxes$  do
3:     if not INTERSECT( $b$ ,  $textboxes$ ) then
4:       DELETE  $b$ 
5:     if INTERSECT( $b$ ,  $textboxes$ ) then
6:        $b.bounding\_box = \text{MAX}(b.bounding\_box, \text{textbox}.bounding\_box)$ 
7:     if INTERSECT( $b$ ,  $cellboxes$ ) then
8:        $b.bounding\_box = \text{MAX}(b.bounding\_box, \text{cellbox}.bounding\_box)$ 
9: procedure ASSIGN CELL ROW AND COLUMN LOCATION
10:  while not INTERSECT( $b$ ,  $cellboxes$ ) do
11:     $b.x1 \leftarrow b.x1 - 5$ 
12:     $b.x2 \leftarrow b.x2 + 5$ 
13:  for  $b$  in  $cellboxes$  do
14:     $num_{col} \leftarrow \text{MAX}(\text{CNT\_INTERSEC}(b.mid_x, cellboxes), num_{col})$ 
15:     $num_{row} \leftarrow \text{MAX}(\text{CNT\_INTERSEC}(b.mid_y, cellboxes), num_{row})$ 
16:     $alignment_x, alignment_y \leftarrow \text{GET\_XY\_ALIGNMENT}(cellboxes)$ 
17:  for  $b$  in  $cellboxes$  do
18:     $b.align_x \leftarrow \text{ALIGN\_DATA}(b.x1, b.mid_x, b.x2, alignment_x)$ 
19:     $b.align_y \leftarrow \text{ALIGN\_DATA}(b.y1, b.mid_y, b.y2, alignment_y)$ 
20:   $col_{pos_x} \leftarrow \text{KMeans}(cellboxes.align_x, num_{col})$ 
21:   $row_{pos_x} \leftarrow \text{KMeans}(cellboxes.align_y, num_{row})$ 
22:  for  $b$  in  $cellboxes$  do
23:     $b.col \leftarrow \text{ALIGN\_TO\_COL}(b.align_x, col_{pos_x}, alignment_x)$ 
24:     $b.row \leftarrow \text{ALIGN\_TO\_ROW}(b.align_y, col_{pos_y}, alignment_y)$ 
25: procedure ASSIGN TEXT LINES TO TABLE
26:  for  $b$  in  $textboxes$  do
27:    if INTERSECT( $b$ ,  $cellboxes$ ) then
28:       $b.col \leftarrow \text{cellbox}.col$ 
29:       $b.row \leftarrow \text{cellbox}.row$ 
30:    else
31:       $b.col \leftarrow \text{ALIGN\_TO\_COL}(b.align_x, col_{pos_x}, alignment_x)$ 
32:       $b.row \leftarrow \text{ALIGN\_TO\_ROW}(b.align_y, col_{pos_y}, alignment_y)$ 
33: procedure SPLIT CELL TEXT LINES WHEN NEIGHBOR IS EMPTY
34:  for  $r$  in  $num_{row}$  do
35:    for  $c$  in  $num_{col}$  do
36:      if IS_EMPTY( $r$ ,  $c$ ) then
37:         $neighbor_{text} \leftarrow \text{GET\_CELLS}(r - 1, c) + \text{GET\_CELLS}(r + 1,$ 
38:         $c)$ 
39:        for  $b$  in  $neighbor_{text}$  do
40:           $b.col \leftarrow \text{ALIGN\_TO\_COL}(b.align_x, col_{pos_x}, alignment_x)$ 
41:           $b.row \leftarrow \text{ALIGN\_TO\_ROW}(b.align_y, col_{pos_y}, alignment_y)$ 
```

---

## 4 Additional cell detection examples

Skill domain and aspect	All items		New items		Total items	
	Number	Percent	Number	Percent	Number	Percent
<b>Total items</b>	135	100	66	100	201	100
<b>Purposes of reading</b>						
Literacy experiences	72	53	33	50	105	52
Strategic use of information	63	47	33	50	96	48
<b>Processes of comprehension</b>						
Focus on and retrieve explicitly stated information	53	39	24	36	77	38
Make straightforward inferences	58	43	25	38	83	41
Integrate and synthesize ideas and information	39	29	18	27	57	28
Examine and evaluate content, language, and textual elements	16	12	8	12	24	12

Content domain and process	All items		New items		Total items	
	Number	Percent	Number	Percent	Number	Percent
<b>Total items</b>	135	100	66	100	201	100
<b>Purposes of reading</b>						
Literacy experiences	72	53	33	50	105	52
Acquire and use information	63	47	27	41	90	45
<b>Processes of comprehension</b>						
Focus on and retrieve explicitly stated information	53	39	14	21	67	33
Make straightforward inferences	46	34	20	30	66	33
Integrate and synthesize ideas and information	38	28	18	27	56	28
Examine and evaluate content, language, and textual elements	18	13	8	12	26	13

Faculty cluster	Population size	Sample size
Sciences	1269 (19.9%)	101(20.4%)
Social Sciences	3212 (50.6%)	247(50.0%)
Humanities	1168 (18.4%)	95(19.3%)
Civil Sciences	705 (11.1%)	51(10.3%)

Sample Group	Some Year 1 Head Start Participation	No Year 1 Head Start Participation	Total
<b>All Randomly Assigned (N=4,667)</b>			
<b>3-Year-Old Cohort</b>			
Head Start Group	85.1%	14.9%	100%
Control Group	17.3%	82.7%	100%
<b>4-Year-Old Cohort</b>			
Head Start Group	79.8%	20.2%	100%
Control Group	13.9%	86.1%	100%

Sample Group	Some Year 1 Head Start Participation	No Year 1 Head Start Participation	Total
<b>Sample Group All Randomly Assigned (N=4,667)</b>			
3-Year-Old Cohort Head Start Group	85.1%	14.9%	10
Control Group	17.3%	82.7%	10
4-Year-Old Cohort Head Start Group	79.8%	20.2%	10
Control Group	13.9%	86.1%	10

Figure 2: Additional cell boundary to structure examples

	THRESHOLD FOR RELEASES			Number of financial companies	% of companies analysed	Number of financial companies on FTSE Europe (top 100)	% of FTSE 100
	to air kg/year	to water kg/year	to land kg/year				
Asbestos	0	12 million	2 million	0 reclassifications	0%	0	0%
Chlorides (as total Cl)	0	2,000	2,000	1 reclassification	2%	1	1%
Cyanides (as total CN)	0	50	50	2 reclassifications	11%	2	5%
Fluorides (as total F)	150,000	5	5	2 reclassifications	11%	2	5%
Particulate matter (PM10)	0	50,000	50,000	2 reclassifications	11%	2	5%
Total Nitrogen	0	5,000	5,000	0 reclassifications	0%	0	0%
Total Phosphorus	0	5,000	5,000	0 reclassifications	0%	0	0%
				Total	100	22	22%

(a) Correct cell detection

(b) Oversplit cell detection

Proportion	Design effect						
	1.7	1.8	1.9	2.0	2.5	3.0	3.5
0.99	1,360	1,440	1,520	1,600	2,000	2,400	2,800
0.95	272	288	304	320	400	480	560
0.90	136	144	152	160	200	240	280
0.85	91	96	101	107	133	160	187
0.80	68	72	76	80	100	120	140
0.75	54	58	61	64	80	96	112
0.56	51	54	57	60	75	90	105
0.55	51	54	57	60	75	90	105
0.50	51	54	57	60	75	90	105
0.45	51	54	57	60	75	90	105
0.26	51	54	57	60	75	90	105
0.25	54	58	61	64	80	96	112
0.20	68	72	76	80	100	120	140
0.15	91	96	101	107	133	160	187
0.10	136	144	152	160	200	240	280
0.05	272	288	304	320	400	480	560
0.01	1,360	1,440	1,520	1,600	2,000	2,400	2,800

(c) Missing Cell detection

Variable	Mean	Std. Dev.	Min	Max
Age	50.8	15.9	21	90
Men	0.47	0.50	0	1
East	0.28	0.45	0	1
Rural	0.15	0.36	0	1
Married	0.57	0.50	0	1
Single	0.21	0.40	0	1
Divorced	0.13	0.33	0	1
Widowed	0.08	0.26	0	1
Separated	0.03	0.16	0	1
Partner	0.65	0.48	0	1
Employed	0.55	0.50	0	1
Fulltime	0.34	0.47	0	1
Parttime	0.20	0.40	0	1
Unemployed	0.08	0.28	0	1
Homemaker	0.19	0.40	0	1
Retired	0.28	0.45	0	1
Household size	2.43	1.22	1	9
Households with children	0.37	0.48	0	1
Number of children	1.67	1.38	0	8
Lower secondary education	0.08	0.27	0	1
Upper secondary education	0.60	0.49	0	1
Post secondary, non tert. education	0.12	0.33	0	1
First stage tertiary education	0.17	0.38	0	1
Other education	0.03	0.17	0	1
Household income (Euro/month)	2,127	1,389	22	22,500
Gross wealth - end of 2007 (Euro)	187,281	384,198	0	7,720,000
Gross financial wealth - end of 2007 (Euro)	38,855	114,128	0	2,870,000

(d) Overmerged cell detection